Default

Request Date: 13-DEC-2010
Expiration Date: 16-DEC-2010
ILL Number:
ILL Number: 4276205
Call Number: SIO 1 IN719;SIO 1 IN719 v.1;SIO 1 IN719 v.2;SIO 1 IN719 v.3;SIO 1 IN719 v.4;SIO 1 IN719 v.5;SIO 1 IN
Format: Article Printed
Title: International journal of offshore and polar engineering /
Article Author: Raoof, M., and Huang, Y. P.: Cyclic Bending Characteristics of Sheathed Spiral Strands in Deep Water Applications
Volume/Issue: 3 3, 3, 3
Part Pub. Date: September 1993
Pages: 189-196
Pub. Place: Golden, Colo. : International Society of Offshore and Polar Engineers, c1991-
Borrower: USD0

Printed Date: 13-DEC-2010
TGQ or OCLC #:
TGQ or OCLC #: 4276204
ID: USD0

ISBN/ISSN: 10535381

Address: CSU Moss Landing Marine Labs/Library/8272 Moss Landing Road/Moss Landing, CA 95039

Patron Name: Chaffey, Mark
Patron e-mail:
Service Level:
Delivery Method: Odyssey preferred (206.107.42.250), Tricor (CSU),
Request Notes: Please don't send directly to patron/ MLML is a part of the California State University System. FAX/ARIEL:(831)632-4403 EMAIL:library@mlml.calstate.edu OCLC Req. Ex. Source: ILLiad
Need By:
Verification Source: <TN:9651><ODYSSEY:mlml.calstate.illiad.oclc.org/ILL> OCLC
Supplier Reference:
Supplier Reference: ILLNUM:71999647
Local request number: ILLNUM:71999647
Owned By: UCSD SIO Library

Service Type: Copy non returnable
Max Cost: USD20

Payment Type: IFM

IFM TRANSACTION $11.00

Copyright Info: US:CCL

Requester Symbol: OCLC:MFL

Return To: ATTN: Interlibrary Loan - Borrowing / Geisel Library / University of California, San Diego / 9500 Gilman Dr. 0175-U / La Jolla, CA 92093-0175 / U.S.A. / ARIEL: 132.239.88.36 / FAX: 858-534-4970 / scrippsill@ucsd.edu

International Journal of Offshore and Polar Engineering
Vol. 3, No. 3, September 1993 (ISSN 1053-5381)

Cyclic Bending Characteristics of Sheathed Spiral Strands in Deep Water Applications

Mohammed Raoof and Yu Ping Huang
School of Architecture and Civil Engineering, South Bank University, London, United Kingdom

ABSTRACT

Straightforward design formulations are given for determining some nonlinear free-bending characteristics of axially preloaded and large-diameter sheathed spiral strands experiencing high external hydrostatic pressure in, for example, deep water floating platform applications. The proposed simple formulations provide means of estimating bounding solutions to strand plane-section bending stiffness, (EI)eff, and hysteresis plus associated critical imposed radii of curvature for any assumed level of external hydrostatic pressure. The practical limitations of the theoretical formulations are discussed in some detail in the light of recent experimental findings in related areas.

INTRODUCTION

Fairly recently, the cable manufacturers have offered high-density and supposedly impermeable polythene sheaths for corrosion protection of large-diameter spiral strands in very deep water applications. Under such conditions, the clench forces caused by the hydrostatic water pressure may become significant compared with the clench forces inside the cable caused by the mean axial load in, say, a guyed tower platform application.

Such external pressures on a sealed multilayered spiral strand will tend to suppress the relative slippage of wires in the cable by increasing the frictional forces between them. A higher strand axial (Raoof, 1989a) and torsional (Raoof, 1990a, 1990b) stiffness will then follow. Moreover, such external pressures may also lead to significant reductions in the axial and restrained bending fatigue life of sheathed spiral strands (Raoof, 1990, 1991a, 1991b, 1992d).

The basis of the free-bending theoretical model for both sheathed and unsheathed and axially preloaded spiral strands has already been reported in some detail elsewhere (Raoof and Huang, 1992a, 1992c) where related work by others has also been cited. As discussed by Raoof (1990a), due to the presence of significant frictional forces between the individual helical wires in a strand, for large enough radii of curvature, initiation of interwire slippage can be totally suppressed and the whole strand effectively behaves as a solid rod (with allowance given for the presence of gaps between the wires). Such conditions are referred to as the no-slip (elastic) case. With decreasing curvature, wires in line-contact in various layers (Fig. 1) will gradually undergo frictional transition from no-slip to full-slip condition (and beyond) with an associated decrease in the effective overall strand plane-section effective bending stiffness under cyclic loading accompanied by significant variations in overall hysteresis. The case when all the wires in line-contact have experienced full slippage is, on the other hand, referred to as the full-slip case.

Previous work by others has largely ignored the presence of interwire friction (e.g., Nowak, 1974; Costello and Butson, 1982),

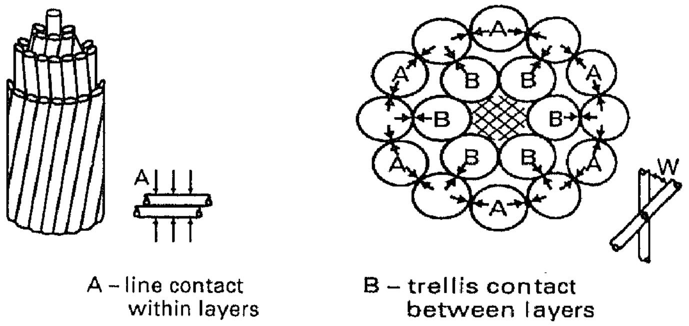

Fig. 1 Pattern of interwire/interlayer contact forces in spiral strands

although some encouraging progress has been made by Lutchansky (1969), Huang (1978), Leclair (1989), Lanteigne (1985) and Feld et al. (1991) to include the effect of interwire friction in their analytical models. A comprehensive review of the frictionless theories is presented by Costello (1990). In view of space limitations, there is little point in attempting a comprehensive literature survey here, particularly when others (Bridge, 1992) have made such surveys very recently. It is, perhaps, worth noting that to the authors' knowledge, none of the published papers, apart from those by the first author, have examined (either theoretically or experimentally) the influence of external hydrostatic pressure on various overall characteristics of sheathed cables.

Apart from a brief description of the salient features of the theory, there is little point in repeating here the often lengthy theoretical derivations or extensive large-scale and carefully conducted experimental work on unsheathed strands, particularly in view of space limitations, and the fact that they have been covered fully elsewhere. Instead, much attention will be devoted to presenting rather straightforward methods for obtaining reliable estimates of various strand free-bending characteristic parameters. These include the no-slip and full-slip plane-section bending stiffnesses

Received December 22, 1992: revised manuscript received by the editors June 21, 1993. The original version (prior to the final revised manuscript) was presented at the Second International Offshore and Polar Engineering Conference (ISOPE-92), San Francisco, June 14-19, 1992.
KEY WORDS: Cable, damping, offshore platforms, vibration, bending.

Parameters	Range of parameters
cable diameter, d (mm)	$16.4 \le d \le 184$
number of layers, N	$2 \le N \le 11$
number of wires in each layer, n	$12 \le n \le 74$
total number of wires, N_T	$16 \le N_T \le 552$
lay angle, α (degrees)	$11 \le \alpha \le 25$
wire diameter, D (mm)	$2.36 \le D \le 6.55$

Table 1 Range of various strand parameters used in study

and maximum specific damping ratio, ψ_{max}, under continued uniform cyclic loading and also the associated critical values of the radii of curvature for which such estimates of bending stiffness and hysteresis may be used in design. It must be noted that the simple proposed methods are based on a comprehensive series of theoretical parametric studies using an extensive range of cable (and wire) diameters and lay angles, the details of which may be found elsewhere (Raoof and Huang, 1992b), and whose outcome in terms of the proposed design methods is briefly presented in what follows. Table 1 presents the range of parameters covered in the theoretical parametric study. Full constructional details of the strands used in the study are presented in Raoof and Huang (1993a). Such design recommendations will be accompanied by a critical discussion of possible practical limitations of the theoretical model, in the light of previously reported experimental findings in related areas.

THEORY

Wire Kinematics Under Plane-Section Bending

Full details of the theoretical parametric study for the axial case may be found in Raoof (1991c) and Raoof and Huang (1993), where it is shown that for a spiral strand under a mean axial strain, S'_1, the interwire line-contact tensorial shear strain, S_{6T}, with corresponding lay angle, α, may be obtained from:

$$\frac{S_{6T}}{S'_1}=0.0196\alpha-0.000394\alpha^2+0.0000247\alpha^3$$
$$=f(\alpha) \qquad \alpha\le 25° \tag{1}$$

where α in Eq. 1 is expressed in degrees. Under plane-section bending, on the other hand, the line-contact slippage, Δu_i, at a polar angle, ϕ (with ϕ= 90°, at the extreme fibre position), in layer i may thus be obtained from Fig. 1:

$$\Delta u_i=2D_iS^i_{6T} \tag{2a}$$
$$=2D_iS'_1f(\alpha_i) \tag{2b}$$

or

$$\Delta u_i=\frac{2D_ir_if(\alpha_i)}{\rho}\sin\phi \tag{2c}$$

where D_i, r_i = wire and helix radii in layer i, respectively, and ρ = the imposed radius of curvature.

Note that Eqs. 1 and 2 take geometrical nonlinearities due to changes in lay angle and helix radius fully into account.

Strand Plane-Section Bending Stiffness Prediction

As discussed by Raoof and Hobbs (1988b), for a strand with its ends fixed against rotation, the elastic constants of the individual orthotropic sheets (layers of wires) along their principal direction of orthotropy may be transferred by the usual rules to the direction corresponding to the strand's axis.

For an axially preloaded spiral strand undergoing plane-section bending, the compliances under sustained uniform cyclic loading along the principal direction of orthotropy are given by:

$$S_{11}=\frac{4}{\pi E_s} \tag{3}$$

$$S_{12}=-\nu S_{11} \tag{4}$$

$$S_{22}=\frac{1}{E_s}\left(0.11+0.59\ln\frac{E_sD}{p}\right) \tag{5}$$

$$S_{66}=\frac{S_{22}}{1-\nu}\left(1-\frac{\Delta_l}{2\Delta_{l\max}}\right)^{-1/2} \tag{6}$$

Note that S_{11} and S_{12} are independent of the strand loading while S_{22} (the normal compliance between wires in line-contact) is only dependent on the magnitude of the normal contact force per unit length of line-contact, p, as determined by the level of strand mean axial load. The line-contact shear compliance, S_{66}, depends on the level of mean axial load by virtue of the term, Δ_{lmax}, given by:

$$\Delta_{l\max}=\frac{3\mu pS_{22}}{4(1-\nu)} \tag{7}$$

where μ is the coefficient of friction, and ν denotes Poisson's ratio. The other parameter, Δ_l in Eq. 6 is the magnitude of the line-contact relative displacement given by Eq. 2 with Δ_l,i= Δu_i. It is noted that Eq. 6 holds for $\Delta_l < 2\,\Delta_{lmax}$ with S_{66} tending to ∞ at the limit. For larger Δ_l, S_{66} is taken as ∞.

The desired layer axial stiffness, $(T'_1/S'_1)_i$, in layer i, may thus be obtained by the transformations given elsewhere (Raoof and Hobbs, 1988b), where T'_1 is the component of normal stress in the layer along the strand axis whose corresponding axial strain is S'_1.

The total bending moment on the strand is:

$$M=\sum_{i=1}^{N}M_i \tag{8a}$$
$$=\frac{(EI)_{eff}}{\rho} \tag{8b}$$

where M_i is the contribution from layer i with a total of N layers in the strand with the outer layer being denoted by i = 1. M_i is given by:

$$M_i=\int_{\infty}^{\rho}\frac{B_i}{\rho^2}d\rho \tag{9}$$

where

$$B_i=\int_0^{2\pi}\left\{E^i_{eff}\left[\left(r_i+\frac{D_i}{2}\right)^4-\left(r_i-\frac{D_i}{2}\right)^4\right]\frac{\sin^2\phi}{4}\right\}d\phi \tag{10}$$

and

$$E^i_{eff}=\left(\frac{T'_1}{S'_1}\right)_i \tag{11}$$

Note that E^i_{eff} is a function of the polar angle ϕ. In the above, r_i is the helix radius in layer i whose associated wire diameter is D_i and the strand is assumed to undergo reversed cyclic bending to a constant radius of curvature, $\pm\rho$.

Plane Section Bending Hysteresis

Full details of the theoretical model are given elsewhere (Raoof and Huang, 1992a, 1992c) and there is little point in repeating the formulations here. Very briefly, in a multilayered strand, the energy dissipation per unit length of layer i, ΔE_i, is given by:

$$\Delta E_i = \sum_{j=1}^{n} \frac{\Delta E_{ij}}{\cos\alpha_i} \tag{12}$$

where ΔE_{ij} is the dissipated energy per unit length of line-contact between wires j and $j+1$ in layer i.

Total strand hysteresis, ΔU, per unit length of spiral strand with a total of N layers is:

$$\Delta U = \sum_{i=1}^{N}\sum_{j=1}^{n} \frac{\Delta E_{ij}}{\cos\alpha_i} \tag{13}$$

Summing all over layers, with n wires in layer i.

The energy input per cycle per unit length of strand, on the other hand, is:

$$U = \frac{M}{2\rho} \tag{14}$$

The specific damping, ψ, is then defined as:

$$\psi = \frac{\Delta U}{U} \tag{15}$$

Note that specific damping is amplitude-dependent and all of the above formulations apply to the case of reversed cyclic free bending of axially preloaded spiral strands experiencing plane-section bending throughout the bending cycle. However, the plane-section bending assumption is only a reasonable one for large radii of curvature (Raoof, 1989b) in, for example, certain applications such as vortex-shedding instabilities where the maximum amplitudes of vibration are of the order of one strand diameter. Raoof and Huang (1992a) investigated the possibility of plane-sections not remaining plane for small radii of curvature, where interlayer slippage can take place with rather drastic reductions in the effective bending stiffness, $(EI)_{eff}$, when compared with that based on the plane-section bending assumption.

DESIGN RECOMMENDATIONS

Bending Stiffness

Fig. 2a presents variations of the effective bending stiffness, $(EI)_{eff}$, of an axially preloaded sheathed 102-mm O.D. spiral strand with the imposed radius of curvature, ρ, and various levels of water depth (representing external hydrostatic pressure) assuming a coefficient of friction $\mu = 0.12$ (Raoof, 1990c). The assumed level of mean axial load on the strand undergoing reversed cyclic bending is 2.3MN, corresponding to a mean axial strain, $\varepsilon_c = 0.00235$. Similar plots for a mean axial tension of 4.6MN are presented in Fig. 2b.

Results in Figs. 2a and b show that strand $(EI)_{eff}$, with plane-section bending assumption, varies between upper (no-slip) and

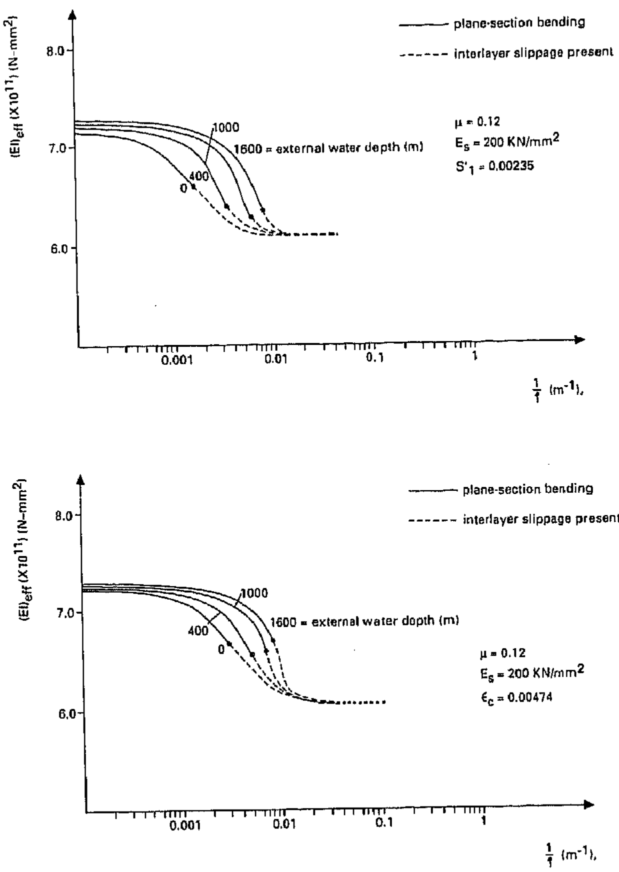

Fig. 2 Variation of effective bending stiffness, $(EI)_{eff}$, in a 102-mm O.D. sheathed spiral strand with imposed radius of curvature and various levels of water depth: (a) mean axial load = 2.3 MN; (b) mean axial load = 4.6 MN

lower (full-slip) bounds, with the external pressure having some influence on the nature of transition between the two bounds. The no-slip limit of $(EI)_{eff}$ is, for all practical purposes, very nearly independent of the magnitude of external pressure and level of mean axial load. It then follows that the simple design recommendations of Raoof (1989b) for spiral strands operating in the absence of hydrostatic pressure may also be used to obtain very reasonable estimates of no-slip and full-slip bounds to $(EI)_{eff}$, with minimal effort.

For either the no-slip or full-slip line-contact of wires, the overall bending rigidity is expressed in the form $E_{eff}I$, where

$$I = \left(\frac{\pi}{4}\right)\left(\frac{\pi d^4}{64}\right) \tag{16}$$

if d is the strand outer diameter and $\pi/4$ caters for the presence of gaps within the wires. Then E_{eff} is a weighted mean of the layer stiffnesses:

$$E_{eff} = \sum_i \lambda_i E_i \tag{17}$$

where

$$\lambda_i = \frac{I_{ni}}{I_o} \tag{18}$$

with

$$I_{ni}=\left[\frac{\pi}{4}\right]\left[\frac{\pi}{64}\right]\left[(2r_i+D_i)^4-(2r_i-D_i)^4\right] \tag{19}$$

and

$$I_o=\sum_i I_{ni} \tag{20}$$

In the above, r_i is the theoretical helix radius for the layer i, calculated by Phillips and Costello (1973).

$$r_i=\frac{D_i}{2}\left[1+\frac{\tan^2\left(\frac{\pi}{2}-\frac{\pi}{n_i}\right)}{\cos^2\alpha_i}\right]^{1/2} \tag{21}$$

where D_i is the wire diameter, and n_i denotes the number of wires in layer i whose lay angle is α_i.

For the full-slip case, E_i in Eq. 17 may then be calculated from Raoof and Huang (1992b).

$$\frac{E_i^{full-slip}}{E_s}=-0.26442-2.004046H_i+6.5735\,H_i^2-3.3068H_i^3$$
$$0.70\le H_i\le 1.0 \tag{22}$$

where E_s is Young's modulus for steel and H_i is given by:

$$H_i=\cos^4\alpha_i \tag{23}$$

Turning to the no-slip case, the following fitted polynomial provides simple means of finding the corresponding no-slip E_{eff} in Eq. 17:

$$\Gamma_i=3.998-7.916k_1+7.238k_1^2-2.321k_1^3$$
$$0.35\le k_1\le 1.0 \tag{24}$$

where

$$\Gamma_i=\frac{E_i^{no-slip}}{E_i^{full-slip}} \tag{25}$$

and

$$k_1=\frac{E_i^{full-slip}}{E_s} \tag{26}$$

Calculation of $E_{eff}I$ is, therefore, as follows:

(i) For any given spiral strand construction, calculate H_i (Eq. 23) for each individual layer i whose lay angle is α_i.

(ii) Using Eq. 22, evaluate the full-slip orthotropic E-values for individual layers i. The corresponding no-slip E-value for individual layers i may be obtained from Eqs. 24~26.

(iii) Eqs. 21, 19, 18 and 17, respectively, may then be used to obtain the strand's overall effective E-value, E_{eff}.

Fig. 3 presents the threshold (critical) radius of curvature, ρ_{min}, at which $(EI)_{eff}$ is 1-5% higher than the plane-section full-slip case, for a wide range of strand mean axial loads and levels of hydrostatic pressure on a sealed spiral strand (Raoof and Huang, 1992b): It is shown that, in general, ρ_{min}/d ratio for any type of strand construction with outer diameter, d, is a function solely of strand mean axial strain, S'_1. Results in Fig. 3 correspond to any type of strand construction whose associated bending stiffness for a given, S'_1, is about 102% of the full-slip $(EI)_{eff}$. The equation describing each individual curve in Fig. 3 is of the form:

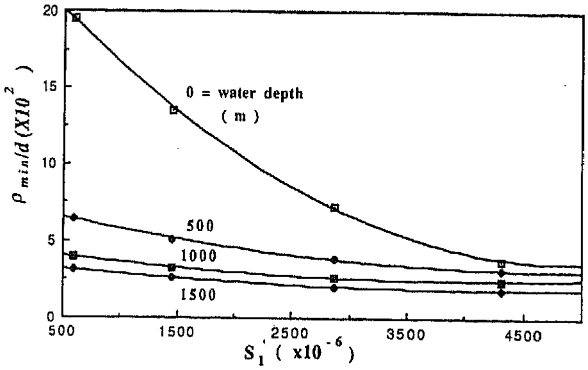

Fig. 3 Variation of ρ_{min}/d for which $(EI)_{eff}/(EI)_{full-slip}$ = 102%, as a function of strand mean axial strain, S'_1, and various levels of water depth (representing external hydrostatic pressure), for any type of sheathed spiral strand construction

$$\frac{\rho_{min}}{d}=A_1+B_1(S_1')+C_1(S_1')^2 \tag{27}$$

where the individual coefficients A_1, B_1, and C_1 may be obtained from Table 2. Intermediate values of ρ_{min}/d for other levels of water depth may be obtained by interpolation.

Fig. 4, on the other hand, presents the variations of the radius of curvature, ρ_{max}, at which the plane-section bending stiffness deviates slightly from the no-slip value, for a wide range of strand mean axial loads and levels of hydrostatic water pressure on a sheathed spiral strand. In general, results show that the ratio ρ_{max}/d is a function of strand mean axial strain, S'_1, and for a given S'_1, decreases with increasing levels of external water depth. Results in Figs. 3 and 4 may be used for any type of strand construction. Plots in Fig. 4 correspond to cases when the bending stiffness for a given S'_1, is about 99% of the no-slip value.

The equation describing each individual curve in Fig. 4 is of the form:

$$\frac{\rho_{max}}{d}=A_2+B_2(S_1')+C_2(S_1')^2+D_2(S_1')^3 \tag{28}$$

where the individual coefficients A_2, B_2, C_2, and D_2 may be obtained from Table 3. Intermediate cases may be estimated by interpolation.

Water depth (m)	A_1 (x10^2)	B_1 (x10^2)	C_1 (x10^7)
0	24.125	−8413.3	8.602
500	7.310	−1759.5	1.823
1000	4.518	−1044.00	1.285
1500	3.552	−797.42	0.905

Table 2 Values of parameters A_1, B_1, and C_1 in Eq. 27, for various levels of water depth

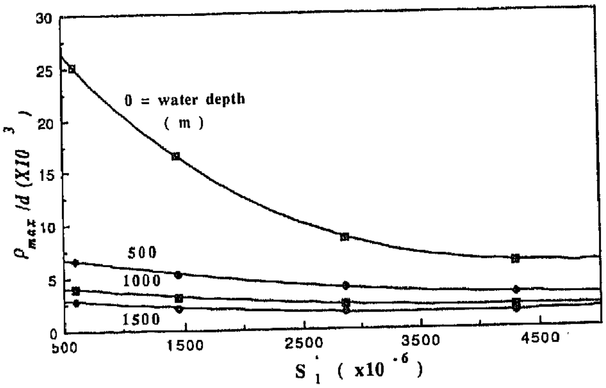

Fig. 4 Variation of ρ_{max}/d at which $(EI)_{eff}$ deviates slightly from no-slip condition, as function of strand mean axial strain, S'_1, and various levels of water depth (representing external hydrostatic pressure), for any type of sheathed spiral strand construction

Water depth (m)	A_2 ($\times 10^3$)	B_2 ($\times 10^3$)	C_2 ($\times 10^8$)	D_2 ($\times 10^{11}$)
0	33.457	−15510	29.070	−1.792
500	7.686	−1880.75	1.955	0
1000	4.625	−1191.82	1.373	0
1500	3.354	−1041.18	1.428	0

Table 3 Values of the coefficients A_2, B_2, C_2 and D_2 in Eq. 28 for various levels of water depth

FREE-BENDING HYSTERESIS

Fig. 5 gives theoretical values of energy dissipation expressed as the specific loss, $\psi = \Delta U/U$, where ΔU is the overall energy dissipation per cycle and U is the strain energy of oscillation,as a function of the radius of curvature, ρ, where cyclic movements occur under $\pm\rho$. The plots in Fig. 5 correspond to five cable constructions with widely different strand (and wire) diameters and lay angles. All of the strands are assumed to be subjected to a mean axial strain, $S'_1 = 0.002867$, and zero water depth. Fig. 5 clearly shows the significant influence of the type of spiral strand construction details on the strand's free-bending damping characteristics.

As discussed fully elsewhere (Raoof and Huang, 1992b), theoretical parametric studies on a wide range of strand constructions — covering strand axial strains, S'_1, in the range $0.0006 < S'_1 < 0.0045$, and water depths ranging from 0 to 1500 m — invariably suggest that the following holds (Fig. 6):

$$\psi_{max} = C\left[\frac{E_{no-slip}}{E_{full-slip}} - 1\right] \tag{29}$$

In the above, $\psi_{max} = (\Delta U/U)_{max}$, is the maximum level of specific damping ratio and the ratio of $E_{no-slip}/E_{full-slip}$ may be obtained as explained previously. Alternatively, Eq. 24 may be used with the proviso that the parameter, k_1, used in this equation now corresponds to the *whole* strand with:

$$k_1 = \frac{E_{full-slip}}{E_s} \tag{30}$$

where $E_{full-slip}$ may be calculated from Eq. 22 with the layer full-slip stiffness, E_i, replaced by the strand overall full-slip stiffness, $E_{full-slip}$, and the parameter $H_i = \cos^4\alpha_i$ replaced by H defined as:

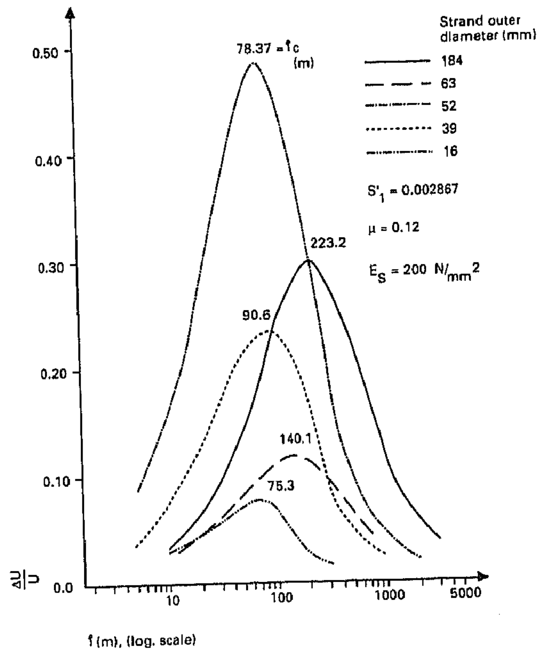

Fig. 5 Theoretical plots of free-bending specific damping, $\psi = \Delta U/U$, as function of imposed cyclic changes in radius of curvature, $\pm\rho$, for a range of strand constructions - zero water depth

$$H = \sum_{i=1}^{N} \frac{I_{ni}}{I_o} \cos^4 \alpha_i \tag{31}$$

where N is the total number of layers, with $i = 1$ referring to the outer layer. I_{ni} and I_o are defined by Eqs. 19 and 20, respectively.

The parameter, C, in Eq. 29 may be obtained from Table 4 with the intermediate values calculated by interpolation. For given

S'_1 ($\times 10^{-6}$)	C	water depth (m)
600	1.086	0
	1.525	500
	1.595	1000
	1.602	1500
1450	1.204	0
	1.624	500
	1.650	1000
	1.675	1500
2867	1.309	0
	1.624	500
	1.707	1000
	1.763	1500
4300	1.384	0
	1.645	500
	1.775	1000
	1.818	1500

Table 4 Values of parameter C in Eq. 29, for various levels of strand mean axial strain, S'_1, and water depth

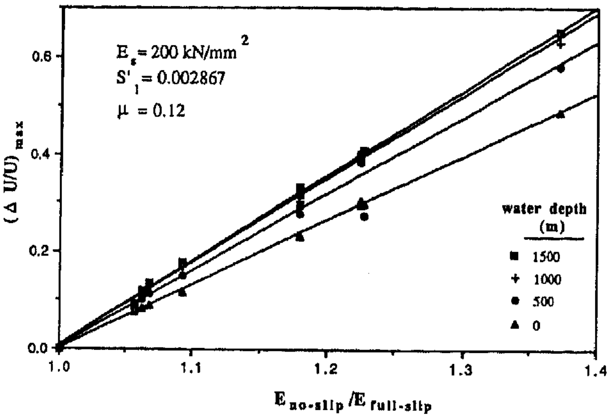

Fig. 6 Relationship between maximum sheathed spiral strand plane-section free-bending maximum specific damping, $\psi_{max} = (\Delta U/U)_{max}$, and parameter $E_{no\text{-}slip}/E_{full\text{-}slip}$, for various levels of strand mean axial strain, S'_1, and water depth - $S'_1 = 0.002867$

strand construction details, therefore, Eqs. 22, 30 and 31 may be used to find the parameter k_1. With k_1 determined, Eq. 24 gives an estimate of the $E_{no\text{-}slip}/E_{\text{full-slip}}$ ratio for the whole strand. Eq. 29 with C-value from Table 4 then gives ψ_{max}.

The other parameter of interest is the critical radius of curvature, ρ_c, associated with which, specific damping, ψ, is a maximum: Yet again, theoretical parametric studies reported fully elsewhere (Raoof and Huang, 1992b) have been used to show that:

$$S'_1\rho_c = a\,\omega^m \tag{32}$$

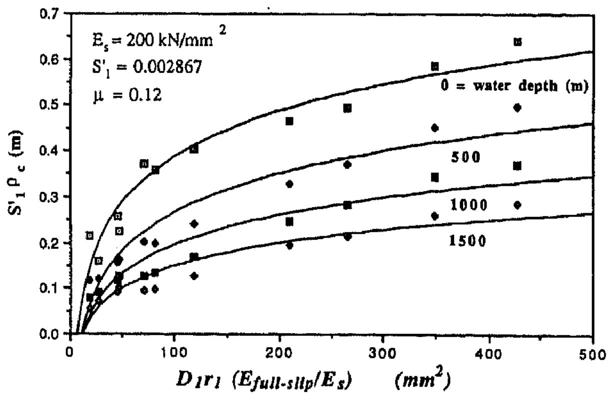

Fig. 7 Plots of parameter $S'_1\rho_c$ against parameter $D_1\ r_1$ ($E_{full\text{-}slip}/E_s$), for various levels of water depth and strand mean axial strain, S'_1, for wide range of sheathed spiral strand constructions - $S'_1 = 0.002867$

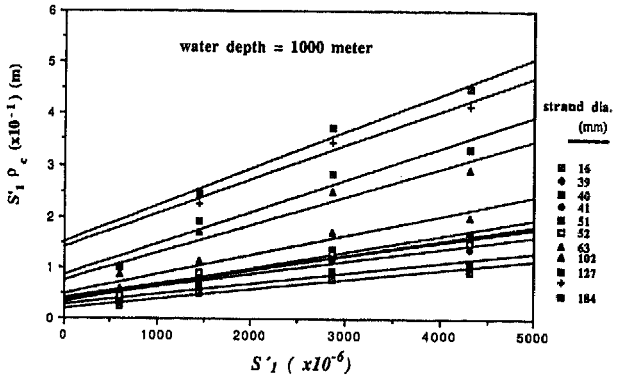

Fig. 8 Variation of parameter $S'_1\rho_c$ as function of strand mean axial strain, S'_1, for various strand constructions - water depth = 1000m

where S'_1 is the mean axial strain and:

$$\omega = D_1 r_1\left(\frac{E_{full\text{-}slip}}{E_s}\right) \tag{33}$$

where D_1 is the wire diameter in the outer layer whose helix radius is r_1, and $E_{full\text{-}slip}$ is the strand overall full slip E-value whose magnitude may be obtained as discussed previously. Fig. 7 shows a typical plot of $S'_1\rho_c$ vs. ω for $S'_1 = 0.002867$ and various levels of water depth.

The constants a and m, for given S'_1, and water depth, are given in Table 5. Moreover, parametric studies have shown that the variation of the term $S'_1\rho_c$ in Eq. 32 with S'_1 is linear and, therefore, for a given, S'_1, it is easy to find the critical value of the radius of curvature, ρ_c: Fig. 8 shows typical plots of $S'_1\rho_c$ vs. S'_1 for a large number of spiral strands with diameters ranging from 16 to 184 mm and experiencing a water depth of 1000 m.

Degradation of Strand Bending Stiffness due to Interlayer Slippage

Work by Raoof and Huang (1992a), based on a corrected and subsequently extended model originally proposed by Lanteigne (1985), provides means of obtaining a bounding solution for determining the gradual reduction of strand-bending stiffness with

S'_1 ($x10^{-6}$)	Water depth (m)	a	m	correlation coefficient R
600	0	0.0587	0.3958	0.89
	500	0.0115	0.4710	0.99
	1000	0.0059	0.4909	0.97
	1500	0.0043	0.4661	0.96
1450	0	0.0576	0.3976	0.94
	500	0.0183	0.4932	0.99
	1000	0.0111	0.5050	0.99
	1500	0.0079	0.5032	0.98
2867	0	0.0546	0.4061	0.95
	500	0.0254	0.4828	0.99
	1000	0.0168	0.5032	0.99
	1500	0.0124	0.5106	0.98
4300	0	0.0529	0.4080	0.96
	500	0.0288	0.4783	0.99
	1000	0.0200	0.5033	0.99
	1500	0.0153	0.5141	0.99

Table 5 Values of parameters a and m in Eq. 32, for various levels of strand mean axial strains, S'_1, and water depth.

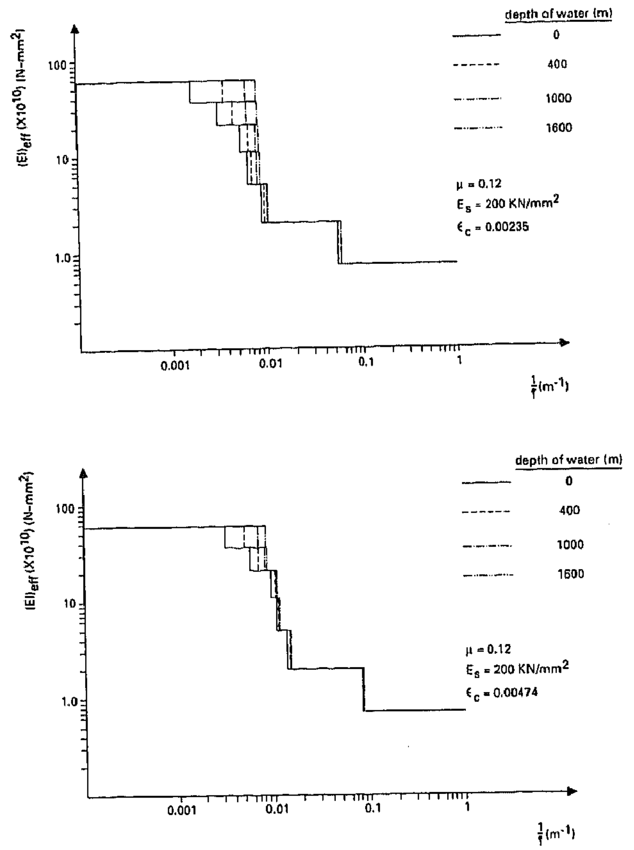

Fig. 9 Variations in flexural rigidity, $(EI)_{eff}$, of 102-mm O.D. sheathed spiral strand as function of applied curvature and external water depth: (a) mean axial load = 2.3MN; (b) mean axial load = 4.6MN

decreasing levels of radii of curvature.

Figs. 9a and b present the way sheathed spiral strands lose their bending stiffness, $(EI)_{eff}$, with reductions in the imposed radius of curvature, ρ, covering a wide range of water depths. Results in Fig. 9a relate to a mean axial load of 2.3MN, while Fig. 9b corresponds to a mean axial load of 4.6MN. It is shown that mean axial load and external water depth can have a profound effect on the magnitude of the radius of curvature at which interlayer slippage in a particular location within the sheathed strand initiates. Results in Figs. 9a and b also identify the range of radii of curvature, ρ, over which the plane-section bending assumption can be applied; deviations from the plane-section bending condition have been shown by dashed lines in the plots of Figs. 2a and b. It must however be noted that initiation of interlayer slippage increases the magnitude of specific damping ratio, $\psi = \Delta U/U$, by increasing ΔU and, at the same time, causing substantial decreases in U: The plane-section bending theory is, therefore, believed to offer a lower bound solution to the value of specific damping for values of ρ below which plane sections do not remain plane during bending.

DISCUSSION

The experimental validation and applicability of the orthotropic sheet concept to large (say, more than 19 wire) strands have already been discussed extensively elsewhere (Raoof and Hobbs, 1988a, 1988b, 1989b, 1990c, 1990d, 1991a, 1991c). In what follows some aspects of the present theory will be discussed in the light of the previously reported large-scale tests on unsheathed strands. It must at once be noted that tests on sheathed strands under high external pressure are very expensive and there is currently no available test results for such cases, although large-scale test results in air reported by others (Claren and Diana, 1969) have been found to provide a very encouraging support for the present bending model for unsheathed cables (Raoof, Huang, 1993b).

Raoof (1990d) has carried out experiments on a newly manufactured 41-mm specimen and has concluded that new strands may need a very lengthy period of axial bedding-in for their internal structure to become stable. During this period complex changes occur in the hysteretic behaviour. The present theory is capable of estimating cable damping in fully bedded-in strands in long-term applications. The damping theory is only developed for continued uniform cyclic loading with the pattern of frictional forces over line-contact patches fully stabilized. As discussed by Hobbs and Raoof (1988a) and Raoof (1990d), torsional tests have indicated that in old and fully bedded-in spiral strands random loading can increase the observed logarithmic decrement by as much as a factor of 4. The effectiveness of random loading in increasing the level of average damping is very much dependent on the level of mean axial load and age of the strand. In new strands the effect of random loading is not so pronounced: The gap between the wires is determined by the manufacturer and, if large enough, can lead to insignificant levels of within-layer hoop forces and hence much reduced hysteresis.

Following the axial and torsional cyclic experiments, it may be assumed that full-slip free-bending stiffness is not so sensitive to age; neither is this property as sensitive to the size of the gaps between the wires in the individual layers as has been widely assumed in previous theoretical studies. No-slip bending stiffness provides an upper bound prediction which will gradually be approached as the spiral strand beds in (Raoof, 1990d).

As shown by large-scale experimental work reported by Raoof and Hobbs (1988a) and Raoof (1990c), for sufficiently small levels of movement the theoretical model for cable hysteresis based on a loading rate-independent Coulomb friction idealization breaks down, and the internal damping of the wire material and the blocking lubricant becomes important. This finding is in accordance with the results of earlier work by others (Johnson, 1961), working on single contacts between elastic spheres.

The present simple method for maximum free-bending damping estimation provides the means of optimizing strand construction details for achieving often desirable increased damping. It is fortunate that substantial increases in damping may be achieved within the manufacturers' current geometrical design limits so that such variations in geometry may not produce adverse effects on other strand characteristics such as axial and/or restrained bending fatigue performance (Raoof, 1991a, 1991b). In general cable free-bending hysteresis is primarily controlled by the choice of the lay angle in various layers, with modest increases in the lay angle leading to significant increases in damping at the cost of slight decreases in the axial stiffness.

CONCLUSIONS

Based on a series of theoretical parametric studies using a newly developed free-bending model for axially preloaded and sheathed spiral strands, it has been possible to present straightforward formulations for determining some aspects of strand free-bending characteristics under sustained cyclic bending to a constant radius of curvature. The new formulations take fully into account the effect of interwire friction in multilayered and large-diameter sheathed spiral strands experiencing external hydrostatic pressure.

It is now possible to obtain with minimal effort reliable estimates of the upper (no-slip) and lower (full-slip) bounds to strand plane-section bending stiffness. Moreover, straightforward techniques are presented for obtaining the magnitude of the radii of curvature associated with which such bounding estimates of bending stiffness may be used in design.

It is shown that cable free-bending hysteresis is largely controlled by the strand construction details, primarily the lay angles in various layers. Modest increases in the lay angle within manufacturers' current design limits can lead to substantial increases in cable damping at the cost of slight reductions in the axial stiffness.

Straightforward formulations are also proposed which offer simple means of predicting the maximum level of specific damping ratio and the associated (critical) radius of curvature at which it is operative. Specific damping ratio of sealed strands is shown to be a function of construction details, level of mean axial load, imposed radius of curvature, and level of externally applied hydrostatic pressure.

Finally, practical limitations of the proposed formulations have been critically discussed in the light of recent experimental findings in related areas.

ACKNOWLEDGEMENTS

Thanks are due to Bridon Ropes personnel, Doncaster, for their patient help with information over a number of years. The authors are also grateful to Mrs. Ada Lam for typing the manuscript.

REFERENCES

Blevins, RD (1977). *Flow-Induced Vibration*, Van Nostrand Reinhold, New York.

Claren, R, and Diana, G (1969). "Mathematical Analysis of Transmission Line Vibration," *IEEE Transactions on Power Apparatus and Systems*, Vol PAS-88, No 12, pp 1741-1771.

Costello, GA, (1990). *Theory of Wire Rope* Springer Verlag, Berlin, Mechanical Engineering Series.

Costello, GA, and Buston, G J (1982). "Simplified Bending Theory for Wire Rope," *J Eng Mech*, ASCE, Vol 114, pp 219-227.

Feld, G, et al. (1991). "Power Cables and Umbilicals Conductor Strain Under Pure Bending," *1st Int Offshore and Polar Eng Conf*, Edinburgh, ISOPE, Vol II, pp 228-235.

Hobbs, RE, and Raoof, M (1984). "Hysteresis in Bridge Strand," *Proc Inst Civ Eng*, Part 2, Vol 77, pp 445-464.

Huang, NC (1978). "Finite Extension of an Elastic Strand with a Central Core," *J App Mech*, Vol 45, pp 852-858.

Johnson, KL (1961). "Energy Dissipation at Spherical Surfaces in Contact Transmitting Oscillating Forces," *J Mech Eng Sci*, Vol 3, pp 362-367.

Lanteigne, J (1985). "Theoretical Estimation of the Response of Helically Armoured Cables to Tension, Torsion, and Bending," *J App Mech*, ASME, Vol 52, pp 423-432.

Leclair, RA (1989). "Upper Bound to Mechanical Power Transmission Losses in Wire Rope," *J Mech Eng*, ASME, Vol 115, No 9, pp 2011-2019.

Lutchansky, M, (1969). "Axial Stresses in Armor Wires of Bent Submarine Cables," *J Eng Ind*, ASME, Vol 91, pp 687-693.

Phillips, JW, and Costello, GA (1973). "Contact Stresses in Twisted Wire Cables," *J Eng Mech Div*, ASCE, Vol 99, pp 331-341.

Raoof, M, and Hobbs, RE (1988a). "Torsion Tests on Large Spiral Strands," *J Strain Analysis*, Inst Mech Eng, Vol 23, No 2, pp 97-104.

Raoof, M, and Hobbs, RE (1988b). "Analysis of Multi-layered Structural Strands," *J Eng Mech Div*, ASCE, Vol 114, pp 1166-1182.

Raoof, M (1989a). "Theoretical Effect of External Pressure on Spiral Strands," *Proc Inst Civ Eng*, Part 2, Vol 87, pp 113-118.

Raoof, M (1989b). "Free Bending Tests on Large Spiral Strands," *Proc Inst Civ Eng*, Part 2, Vol 87, pp 605-626.

Raoof, M (1990a). "Sheathed Spiral Strands in Deep Water Applications," *Int Conf Offshore Mech and Arctic Eng*, Houston, Vol I, Part B, pp 613-622.

Raoof, M (1990b). "Effect of Hydrostatic Pressure on Strand Behaviour," *J Strain Analysis, Inst Mech Eng*, Vol 25, No 2, pp 75-84.

Raoof, M, (1990c). "A Multi-Contact Problem," *Proc 9th Int Conf Experimental Mech*, Lyngby, Denmark, pp 103-111.

Raoof, M (1990d). "Comparison Between the Performance of Newly Manufactured and Well-Used Spiral Strands," *Proc Inst Civ Eng*, Part 2, Vol 89, pp 103-120.

Raoof, M (1991a). "Axial Fatigue Life Prediction of Structural Cables from First Principles," *Proc Inst Civ Eng*, Part 2, Vol 91, pp 19-38.

Raoof, M (1991b). "Cable Fatigue Prediction in Offshore Applications," *Proc Int Conf Offshore Mech and Arctic Eng*, Norway, Vol III, Part B, pp 403-411.

Raoof, M (1991c). "The Prediction of Axial Damping in Spiral Strands," *J Strain Analysis*, Vol 26, No 4, pp 221-229.

Raoof, M, and Huang, YP (1992a). "Free Bending Characteristics of Sheathed Spiral Strands Under Cyclic Loading," *J Struct and Buildings*, Inst Civ Eng, Vol 94, pp 469-484.

Raoof, M, and Huang, YP, (1992b). "Simple Methods for Estimating Various Sheathed Spiral Strand Bending Characteristics," *J Struct and Buildings*, Inst Civ Eng, Vol 94, pp 485-500.

Raoof, M, and Huang, YP (1992c). "Free Bending Hysteresis in Spiral Strands," *2nd Int Offshore and Polar Eng Conf, ISOPE*, San Francisco, Vol II, pp 480-391.

Raoof, M (1992d). "Free Bending Fatigue of Axially Preloaded Spiral Strands," *J Strain Analysis*, Inst Mech Eng, Vol 27, No 3, pp 127-136.

Raoof, M, and Huang, YP (1993a). "Simplified Methods for Analysing Structural Strands," *The Structural Engineer*, Inst Struct Eng, UK, Vol 70, No 22, pp 390-397.

Raoof, M, and Huang, YP, (1993b). "Lateral Vibrations of Steel Cables Including Structural Damping," accepted for pub in *J Struct and Buildings*, Inst Civ Eng, UK, Vol 99, pp 123-133.

Ridge, IML (1992). Bending - Tension Fatigue of Wire Rope, *PhD thesis*, Univ of Reading, UK.